intracellular distribution and the transport of physiologically important ions in cultured cells using cryotechniques.

Semiconductor-grade silicon wafers (General Diode) were used as the substrate for cell growth, since an electrically conducting sample mount is a requirement for ion-microscopic analysis. This substrate is nontoxic and provides cell growth rates and morphologies comparable to those of cells grown on glass cover slips. Dulbecco's modified Eagle's medium with 10 percent calf serum (Gibco) was used for cell growth. Normal rat kidney (NRK) cells were seeded at a density of 3.0×10^5 to 3.5×10^5 cells per 100-mm plastic dish (Falcon) and incubated at 37°C in a 5 percent CO_2 atmosphere. Each petri dish contained approximately ten silicon wafers (*3*). The cells were treated with ouabain in about 4 days, when they had reached confluency. Ouabain (1 m*M*; Sigma) was used to inhibit the Na^+- and K^+-dependent adenosine triphosphatase of the plasma membrane. The samples were collected after 0, 20, and 60 minutes of treatment with ouabain. In preparation for ion-microscopic analysis, these samples were freeze-fixed with liquid nitrogen slush (−206°C), cryofractured under liquid nitrogen by a sandwich technique (*4*), and freeze-dried at −80°C for 24 hours. An ion microscope (Cameca model IMS-3f) operating with an 8.0-KeV O_2^+ primary ion beam and monitoring positive secondary ions was used for this study (*5*). When the Na^+-K^+ ion transport was imaged as a function of time, all instrumental parameters (primary beam density, energy slits, channelplate gain, and so on), image exposure times (1 second), and photographic processing times were kept constant between treatments.

The intracellular distribution of sodium and potassium and Na^+-K^+ ion transport in NRK cells are shown in Fig. 1. At 0 minutes after treatment with ouabain, high potassium and low sodium intensities were observed, for example, as seen in cell A. Within each cell, the intensity of potassium was slightly higher in the nucleus than in the cytoplasm.

Cells sampled after 20 minutes and 60 minutes of ouabain treatment showed an intracellular increase in sodium and loss of potassium with time (Fig. 1). These observations have been confirmed with Chinese hamster ovary cells and 3T3 cells.

Ion images showing cell morphology can be produced for any element (or isotope) of interest. In addition to sodium and potassium, other physiologically important elements such as calcium, magnesium, chloride, and phosphorus

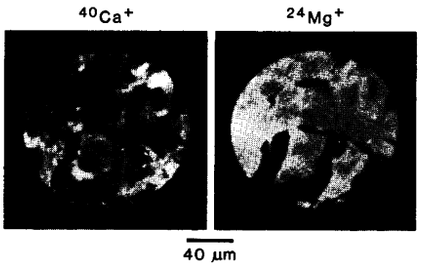

Fig. 2. The ion images of $^{40}Ca^+$ (left) and $^{24}Mg^+$ (right), illustrating the intracellular distribution of calcium and magnesium in freeze-fractured NRK cells.

can also be studied. The distribution of calcium and magnesium in NRK cells as revealed by ion micrographs (Fig. 2) showed that calcium concentrates more in the cytoplasm than in the nuclei of the cells. Even within the cytoplasm calcium is not homogeneously distributed, whereas the distribution of magnesium is almost homogeneous throughout the cell. The intracellular distribution of calcium is markedly different from that of sodium, potassium, and magnesium. This observation has been confirmed in several cell lines. It is known that calcium-binding organelles, such as mitochondria and the endoplasmic reticulum, and calcium-binding proteins are present in the cytoplasm.

The exposure time to produce the images in Fig. 2 was 30 seconds, and the calcium image was recorded first. The longer exposure times were required because of the low intracellular concentrations of these elements. Even after 10 minutes of ion bombardment, no noticeable preferential etching was observed between the nuclei and the cytoplasm of the fractured cells.

The ion microscope is capable of detecting all elements (isotopes) from hydrogen to uranium with sensitivities in the parts-per-million range.

Our results show that ion microscopy, applied to cell culture systems, can be a useful method for studying ion distribution and ion transport under different physiological, pathological, and toxicological conditions.

SUBHASH CHANDRA
GEORGE H. MORRISON
Baker Laboratory of Chemistry,
Cornell University,
Ithaca, New York 14853

References and Notes

1. R. Castaing and G. Slodzian, *J. Microsc. (Paris)* **1**, 395 (1962).
2. G. H. Morrison and G. Slodzian, *Anal. Chem.* **47** (No. 11), 932A (1975).
3. The silicon wafers (approximately 1 cm^2) were washed in deionized distilled water and sterilized before they were seeded with cells. Cells were grown on the polished surface to allow visual examination with a reflected light microscope. The rough sides of the wafers were numbered to identify different treatments.
4. The details of this sandwich technique were presented at the 1984 Annual Conference of the American Society for Cell Biology [S. Chandra *et al.*, *J. Cell Biol.* **99** (No. 4), part 2, 424a (1984).], and a manuscript is in preparation. This technique makes it possible to fracture cells without removing them from the substrate. In addition, it eliminates the need for washing the extracellular nutrient media and cryosectioning before ion microanalysis. Only the fractured cells are used for ion microanalysis.
5. A mass-filtered, 400-nA O_2^+ primary ion beam (diameter, 100 μm) was directed onto a 250 by 250 μm^2 raster. The secondary ions were extracted from a circular region (diameter, 150 μm) centered within the raster.
6. We thank E. Racker for reviews of the ouabain experiment and the manuscript and C. Coulter and the Cornell biophysics facility for culturing cells. Supported by grant R01GM24314 from the National Institutes of Health.

25 January 1985; accepted 5 April 1985

Dissociation of Antitumor Potency from Anthracycline Cardiotoxicity in a Doxorubicin Analog

Abstract. *The search for new congeners of the leading anticancer drug doxorubicin has led to an analog that is approximately 1000 times more potent, noncardiotoxic at therapeutic dose levels, and non–cross-resistant with doxorubicin. The new anthracycline, 3'-deamino-3'-(3-cyano-4-morpholinyl)doxorubicin (MRA-CN), is produced by incorporation of the 3' amino group of doxorubicin in a new cyanomorpholinyl ring. The marked increase in potency was observed against human ovarian and breast carcinomas in vitro; it was not accompanied by an increase in cardiotoxicity in fetal mouse heart cultures. Doxorubicin and MRA-CN both produced typical cardiac ultrastructural and biochemical changes, but at equimolar concentrations. In addition, MRA-CN was not cross-resistant with doxorubicin in a variant of the human sarcoma cell line MES-SA selected for resistance to doxorubicin. Thus antitumor efficacy was dissociated from both cardiotoxicity and cross-resistance by this modification of anthracycline structure.*

The anthracycline doxorubicin has become one of the most important drugs in the treatment of human cancers (*1*). In addition to toxicity against normal proliferating tissues, such as the bone marrow and gastrointestinal tract, anthracyclines are associated with cardiac damage related to both the total dose and the sched-

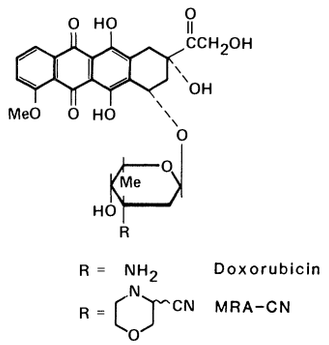

Fig. 1. Structures of doxorubicin and MRA-CN. The synthesis of MRA-CN from doxorubicin was recently described (*5*).

ule of drug administration (*2*). Therapy with anthracyclines is limited not only by this toxicity to normal tissues but also by resistance, which may be present initially or which may emerge during therapy (*3*).

Several hundred analogs of doxorubicin have been synthesized in attempts to structurally separate the various pharmacodynamic effects of the anthracyclines, and in particular to selectively reduce or eliminate their cardiotoxicity (*4*). Some differences in antitumor activity and cardiotoxicity have been suggested among these analogs. However, such differences have not been demonstrated definitely, partly because of minor alterations (less than tenfold) in the molar potency of compounds and difficulties in quantitatively assessing cardiotoxicity.

Recently an analog of doxorubicin was synthesized that was 200 to 1600 times more potent on initial screening in several murine tumors (*5*). The structure of the new compound, 3′-deamino-3′-(3-cyano-4-morpholinyl)doxorubicin (MRA-CN), is illustrated in Fig. 1. We report here the activities of MRA-CN and doxorubicin against several human tumors in vitro, in a doxorubicin-resistant human sarcoma cell line, and in a quantitative model of anthracycline cardiotoxicity, the cultured fetal mouse heart. Our results show a clear separation of the antitumor and cardiotoxic actions of the two anthracyclines by a structural modification of doxorubicin and suggest that MRA-CN may be active against some human cancers that are resistant to doxorubicin.

Figure 2 shows the cytotoxicities of doxorubicin and MRA-CN against a breast and an ovarian carcinoma, as measured by clonogenic assays in soft agar (*6*). MRA-CN was, respectively, 1500 and 150 times more potent than doxorubicin against these two tumors, as assessed by the ratio of the drug concentrations required to inhibit colony formation 50 percent (IC_{50}) (Fig. 2). Nine human tumor specimens were examined, including six ovarian and three breast carcinomas (Table 1). The IC_{50} values ranged from $0.03 \times 10^{-9}M$ to $2.0 \times 10^{-9}M$ for MRA-CN and from $0.3 \times 10^{-6}M$ to $2.0 \times 10^{-6}M$ for doxorubicin. The ratio of the IC_{50}'s of doxorubicin and MRA-CN, an index of the increased potency of MRA-CN, ranged from 100 to 15,000, with a median of 1,000.

The relative potential of MRA-CN and doxorubicin to produce cardiotoxicity was compared in a fetal mouse heart culture system in which anthracyclines produce characteristic morphological changes and release of lactic acid dehydrogenase (LDH) (*7*). This model appears to be specific for anthracyclines in that other anticancer drugs that are noncardiotoxic do not produce these effects. The residual LDH activity in fetal mouse hearts after exposure to MRA-CN and doxorubicin is shown in Fig. 3. A significant decrease in residual cardiac LDH occurred at the highest concentration of both drugs ($P < 0.05$ compared to saline-treated controls, Student's *t*-test). Electron microscopy confirmed that similar cardiac lesions were induced by the two drugs at the higher concentrations, with typical chromatin clumping, mitochondrial disruption, and lysis of myofibrils. Thus the molar potency of MRA-CN was similar to that of doxorubicin in this model.

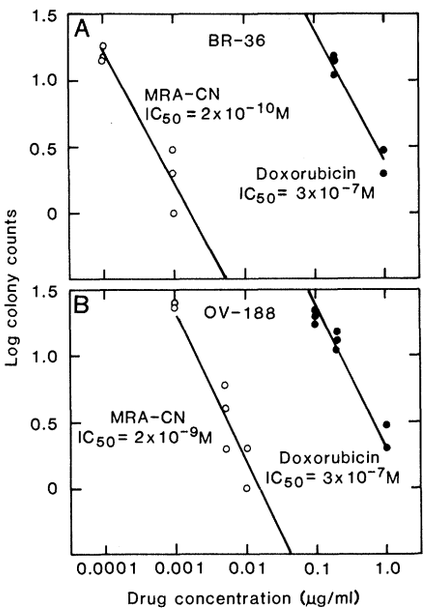

Fig. 2. Dose response curves for doxorubicin and MRA-CN, as determined from soft agar clonogenic assays of (A) a breast carcinoma for which the IC_{50} ratio for doxorubicin to MRA-CN was 1500 and (B) an ovarian carcinoma for which the IC_{50} ratio for doxorubicin to MRA-CN was 150. Tumor specimens from patients were disaggregated by fine mincing and exposure to Pronase-collagenase-deoxyribonuclease (*16*). The cells were exposed to the drugs at various concentrations for 1 hour, washed, and plated in triplicate in a two-layer system of 0.3 percent over 0.5 percent agar in Waymouth's and McCoy's media with 15 percent newborn calf serum. Colonies were counted after 2 to 3 weeks of growth. The data shown are the log transformations of individual colony counts and drug concentrations.

Table 1. Cytotoxicity of doxorubicin and MRA-CN in clonogenic assays of human tumors. Single-cell suspensions of three breast and six ovarian carcinomas were prepared (*16*). The cells were exposed to the drugs at various concentrations for 1 hour, washed, and plated in triplicate in 0.3 percent agar. Colonies were counted after 2 to 3 weeks of growth.

Specimen	IC_{50} (M)		Molar potency*
	Doxorubicin	MRA-CN	
BR-20	5×10^{-7}	3×10^{-11}	15,000
BR-36	3×10^{-7}	2×10^{-10}	1,500
BR-40	2×10^{-6}	1×10^{-9}	2,000
OV-103	2×10^{-7}	2×10^{-9}	100
OV-137	1×10^{-6}	2×10^{-9}	500
OV-169	2×10^{-6}	2×10^{-9}	1,000
OV-182	2×10^{-6}	2×10^{-9}	1,000
OV-186	5×10^{-7}	2×10^{-9}	250
OV-188	3×10^{-7}	2×10^{-9}	150

*Ratio of IC_{50} for doxorubicin to IC_{50} for MRA-CN.

We studied the question of cross-resistance of these two anthracyclines in variants of a human sarcoma cell (*8*). The parent cell line, MES-SA, was recently characterized in our laboratory and is very sensitive to doxorubicin, with an IC_{50} of $2 \times 10^{-8}M$. The subline Dx5, developed by stepwise exposure to doxorubicin, is 100-fold resistant to doxorubicin and displays cross-resistance to several other agents, including dactinomycin, the vinca alkaloids, the epipodophyllotoxins, and daunorubicin, another anthracycline congener of doxorubicin (*9*). MRA-CN does not exhibit cross-resistance with doxorubicin in this model (Fig. 4). As shown by the two curves on the left in Fig. 4, the IC_{50} for MRA-CN in both the sensitive MES-SA cells and the resistant Dx5 cells is $1 \times 10^{-9}M$. The two curves on the right illustrate the effects of doxorubicin in the sensitive and resistant cells, with IC_{50}'s of $2 \times 10^{-8}M$ and $2 \times 10^{-6}M$, respectively.

In summary, MRA-CN represents a major structure-activity modification of anthracyclines. Elaboration of the cyano-morpholinyl moiety at the 3′ position of doxorubicin has resulted in a marked increase in antitumor potency without a corresponding change in cardiotoxicity. This increase in antitumor potency is not entirely selective, however, since in

mice MRA-CN is also 500 to 1000 times more lethal than doxorubicin, probably because of effects on normal proliferating tissues such as the bone marrow (*5*). However, the extreme potency of MRA-CN makes it attractive for selective delivery by methods such as liposomes and monoclonal antibodies (*10*).

It was recently reported that MRA-CN produces interstrand cross-linking of DNA, whereas doxorubicin does not (*11*). This suggests that the cyano-morpholinyl group may be reactive and act as an alkylating moiety. Thus MRA-CN may exhibit a novel mechanism of action to account for its increased cytotoxicity relative to other anthracyclines. The anthracyclines are known to bind to DNA by intercalation (*12*). We postulate that the intense potency of MRA-CN may be due to reactivity of the cyano-morpholinyl group resulting in covalent binding to DNA, thus combining both intercalation and alkylation of DNA in its cytotoxic mechanisms. In this regard, MRA-CN appears to be more specific than doxorubicin as an inhibitor of cellular messenger RNA synthesis (*13*).

MRA-CN may also differ from doxorubicin in its subcellular distribution and binding. Among the chemical properties associated with the structural change in MRA-CN are an increase in lipophilicity and the nonbasicity of the amino nitrogen (*5*).

It has been hypothesized that anthracycline cardiotoxicity results from free radical formation via reduction of the quinone moiety at the anthracycline ring (*14*). Our results showing equivalent cardiotoxicities of doxorubicin and MRA-CN are consistent with this theory, since the quinone group at the anthracycline ring is unchanged in MRA-CN. Substitution of the quinone by an imino group does appear to selectively reduce the cardiotoxicity of doxorubicin without conferring increased cytotoxic potency (*15*).

Caution should be exercised in extrapolating these in vitro results to the clinical setting. The distribution, metabolism, and disposition of MRA-CN might substantially affect its activities in vivo. Because of the extreme potency of this compound and its evident differences from other anthracyclines, detailed toxicological studies will be important.

The cyano-morpholino substituent may itself represent an important lead in the design of cytotoxic agents. Its introduction into the doxorubicin molecule has produced a marked alteration of the biological effects of this anthracycline. Similar substitutions in other intercalating agents as well as other classes of compounds would be of interest.

BRANIMIR IVAN SIKIC
MOHAMED N. EHSAN
W. GRAYDON HARKER
NINA F. FRIEND
BYRON W. BROWN
Stanford University School of Medicine, Stanford, California 94305
ROBERT A. NEWMAN
M. D. Anderson Hospital, Houston, Texas 77030
MILES P. HACKER
University of Vermont, Burlington 05405
EDWARD M. ACTON
SRI International, Menlo Park, California 94025

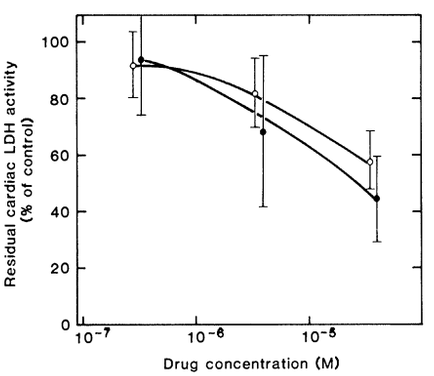

Fig. 3. Cardiotoxicity of doxorubicin (○) and MRA-CN (●), estimated from the percentage of residual LDH activity in cultured fetal mouse hearts after drug exposure. Fetal mouse heart organ cultures were prepared by a modification of the method of Kloner and Ingwall (*17*) as previously described (*7*). After a 24-hour equilibration period doxorubicin, MRA-CN, or an equivalent volume of 0.9 percent NaCl was added to the culture dishes with fresh medium. Hearts were incubated with the drugs for 24 hours, removed, and either prepared for examination by electron microscopy or sonicated in phosphate-buffered 0.9 percent NaCl. Heart sonicate solutions were assayed for LDH activity and protein content (*7*). Values (means ± standard deviations, $n = 6$) are percentages of control LDH activity per milligram of protein. The decreases in LDH produced by both drugs at the highest concentration (34 μM) are significantly different from the results for saline-treated controls ($P < 0.05$, Student's t-test).

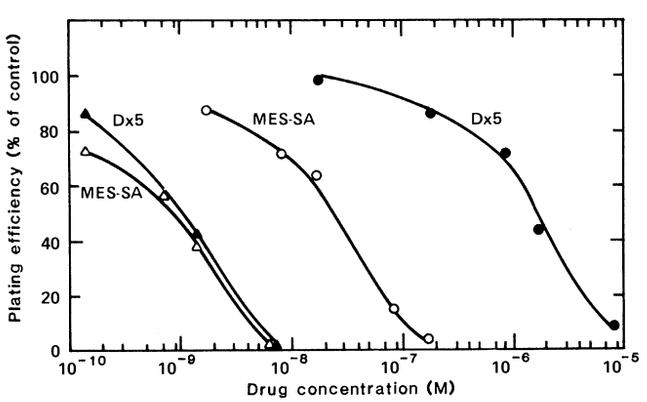

Fig. 4. Lack of cross-resistance between doxorubicin and MRA-CN in a doxorubicin-selected variant of the human sarcoma cell line MES-SA. Dose response curves for doxorubicin and MRA-CN were generated by clonogenic assay in soft agar (*8, 16*). The Dx5 subline of MES-SA cells, developed by continuous exposure to increasing concentrations of doxorubicin, manifests 100-fold resistance to doxorubicin, and resistance to vinca alkaloids, dactinomycin, colchicine, the podophyllotoxins, and the anthracenedione mitoxantrone (*9*). The two curves on the left represent the cytotoxicity of MRA-CN in the MES-SA and Dx5 cell lines. The two curves on the right illustrate the effects of doxorubicin in MES-SA and in Dx5.

References and Notes

1. R. H. Blum and S. K. Carter, *Ann. Int. Med.* **80**, 249 (1974); P. Wiernik, in *Anthracyclines: Current Status and New Developments*, S. T. Crooke and S. D. Reich, Eds. (Academic Press, New York, 1980), pp. 273–294.
2. L. Lenaz and J. A. Page, *Cancer Treat. Rev.* **3**, 111 (1976); D. D. von Hoff *et al.*, *Ann. Int. Med.* **91**, 710 (1979).
3. R. F. Ozols *et al.*, *Cancer Res.* **40**, 2743 (1980).
4. E. M. Acton, in *Anthracyclines: Current Status and New Developments*, S. T. Crooke and S. D. Reich, Eds. (Academic Press, New York, 1980), pp. 15–26.
5. E. M. Acton *et al.*, *J. Med. Chem.* **27**, 638 (1984).
6. S. E. Salmon *et al.*, *N. Engl. J. Med.* **298**, 1321 (1978).
7. M. P. Hacker, R. A. Newman, M. A. Fagan, *Drugs Exp. Clin. Res.* **9**, 393 (1983).
8. W. G. Harker, F. R. MacKintosh, B. I. Sikic, *Cancer Res.* **43**, 4943 (1983).
9. W. G. Harker and B. I. Sikic, *ibid.*, in press.
10. Y. Hashimoto *et al.*, *Cancer Res.* **43**, 5328 (1983); L. D. Leserman, P. Mackey, J. Berbet, *Nature (London)* **293**, 226 (1981); T. D. Heath *et al.*, *Proc. Natl. Acad. Sci. U.S.A.* **80**, 1377 (1983).
11. J. Westendorf, H. Marquardt, H. Marquardt, *Proc. Am. Assoc. Cancer Res.* **25**, 293 (1984).
12. T. Facchinetti *et al.*, *Chem. Biol. Interact.* **20**, 97 (1978); T. W. Plumbridge and J. R. Brown, *Biochim. Biophys. Acta* **563**, 181 (1979); F. Zunino *et al.*, *ibid.* **607**, 206 (1980).
13. J. B. Johnston, B. Habernicht, E. M. Acton, R. I. Glazer, *Biochem. Pharmacol.* **32**, 3255 1983).
14. C. E. Myers *et al.*, *Science* **197**, 165 (1977).
15. G. L. Tong, D. W. Henry, E. M. Acton, *J. Med. Chem.* **22**, 36 (1979).
16. F. R. MacKintosh, T. L. Evans, B. I. Sikic, *Cancer Chemother. Pharmacol.* **6**, 205 (1981).
17. R. A. Kloner and J. S. Ingwall, *Exp. Mol. Pathol.* **32**, 317 (1980).

18. Supported by NIH grants CA 24543, CA 32250, and CA 33303. B.I.S. is a recipient of a faculty development award in clinical pharmacology from the Pharmaceutical Manufacturer's Association Foundation.

14 September 1984; accepted 15 April 1985